Optical nutation induced by transition between levels inside and outside the well in a core–shell CdSe/ZnS quantum dot

2006 J. Phys.: Condens. Matter 18 10989

(http://iopscience.iop.org/0953-8984/18/48/026)

INSTITUTE OF PHYSICS PUBLISHING JOURNAL OF PHYSICS: CONDENSED MATTER

J. Phys.: Condens. Matter **18** (2006) 10989–10998 doi:10.1088/0953-8984/18/48/026

Optical nutation induced by transition between levels inside and outside the well in a core–shell CdSe/ZnS quantum dot

Shaohua Gong and Duanzheng Yao[1]

Department of Physics, Wuhan University, Wuhan 430072, People's Republic of China

E-mail: dzyao@whu.edu.cn

Received 20 June 2006, in final form 7 November 2006
Published 17 November 2006
Online at stacks.iop.org/JPhysCM/18/10989

Abstract

The energy eigenvalues and eigenfunctions of a core–shell CdSe/ZnS quantum dot structure have been obtained under an effective-mass approximation. The electric transition dipole moment induced by the 1s (inside the well)–1s (outside the well) transition has been calculated. The optical nutation signal induced by the transition has been calculated numerically based on the optical Bloch equations. In particular, the influence of the size variation of the core's radius and the shell's thickness has been studied. It has been shown from the results that the optical nutation signal is sensitive to the size and structure, and that there is an optimal structure and size for the optical nutation phenomenon. The quantum size dependent Rabi frequency and intensity of the optical nutation are also discussed.

(Some figures in this article are in colour only in the electronic version)

1. Introduction

The low-dimensional semiconductor structures such as quantum wells (QWs), quantum wires (QWRs) and quantum dots (QDs) have been applied in many optoelectronic materials and devices for optical communication, optical computing and biological probes [1–4]. Their wonderful optical properties, especially the nonlinear optical properties, have attracted the interest of many scientists. Many experimental and theoretical investigations are being carried out [5–7]. Core–shell CdSe/ZnS QDs, which are like a type of wide direct gap semiconductor QD made of II–VI crystal classes, is one such structure under investigation. Its absorption and photoluminescence spectra were studied by Azad Malik *et al* [8] and its conduction mechanism and electroluminescence spectra were studied by Mhikmet and Talapin *et al* [9].

[1] Author to whom any correspondence should be addressed.

The study of transient optical effects like photon echo, free-induction decay and optical nutation has become one of the most important areas of research in this recently developed subfield. Among the different coherent transient phenomena, optical nutation is one of important tools for the study of relaxation mechanisms and hot-carrier effects in semiconductor materials. For example, it is an important approach in the calculation of the matrix elements of transition dipoles and the lifetime of excited states [10, 11].

Normally in experiments on optical nutation a pulsed laser with a sufficiently sharp leading edge is needed and a pulsed Stark-shift technique is used, which allows the observation of the transient nutation, with a cw laser which has a line width much narrow than the Doppler width of the transition. An dc electric field applied to the sample, which is in a Stark cell, can Stark-shift the atoms or molecules in or out of resonance with the cw exciting laser beam. This is equivalent to switching on or off the resonant exciting field, which is initially in resonance with a group of particles. The sudden application of the electric field shifts the resonance to a different group of particles, under the condition that the Stark shift is comparable to the Doppler width. This new group of particles, following the switching on of the field, starts to absorb and gives rise to the observed transient nutation. Due to the remarkable growth of femtosecond (fs) laser technology, we can now observe the phenomenon of optical nutation in QWs, QWRs and QDs of semiconductor materials by using a fs laser.

Optical nutation has been studied in bulk semiconductors using a two-level model by Singh [12]. Sen has studied it in semiconductor QWs and QWRs; even those low-dimensional structures were put into a strong magnetic field [13, 14]. However, there has been little work about optical nutation in core–shell QDs.

In this paper, we make an attempt to investigate theoretically the optical nutation induced by the 1s (inside the well)–1s (outside the well) electronic transition in core–shell CdSe/ZnS QD, employing a two-level model. In particular we have studied the influence of quantum confined effects (QCE) on the optical nutation signal while the inner radius or outer radius of the QD is changed. In addition, we keep the radius of the QD smaller than the exciton Bohr radius of the materials all the time, i.e. it is a strong confined system.

2. Model and theory

Suppose the model is an isolated CdSe/ZnS core–shell quantum dot with inner radius R_1 and outer radius R_2 as shown in figure 1.

We consider it forms a shell well and a centric barrier because the two kinds of materials have different potentials. The potential of the core is chosen to be the zero reference point of energy, and the band-gap of ZnS is wider than that of CdSe, thus $V_c > 0$ [15]. On the premise of the effective mass approximation, the steady Schrödinger equation for electron can be written as

$$\left\{-\frac{\hbar^2}{2m_i^* r^2}\left[\frac{\partial}{\partial r}\left(r^2\frac{\partial}{\partial r}\right)+\frac{1}{\sin\theta}\frac{\partial}{\partial\theta}\left(\sin\theta\frac{\partial}{\partial\theta}\right)+\frac{1}{\sin^2\theta}\frac{\partial^2}{\partial\varphi^2}\right]+V_i(r)\right\}\Phi_{nlm}(r) = E\Phi_{nlm}(r) \tag{1}$$

where $\hbar = h/2\pi$, h is Planck's constant, E is the energy eigenvalue and $\Phi_{nlm}(r)$ is the corresponding eigenfunction. n is the principal quantum number. l and m are the angular momentum quantum numbers. m_i^* is the effective mass of an electron in the ith region. $V_i(r)$ is the potential of the ith region. The values of m_i^* and $V_i(r)$ are relative to the position in the model and are expressed as follows:

$$m_i^* = \begin{cases} m_1^*, & r \leqslant R_1 \\ m_2^*, & R_1 < r \leqslant R_2 \end{cases} \tag{2}$$

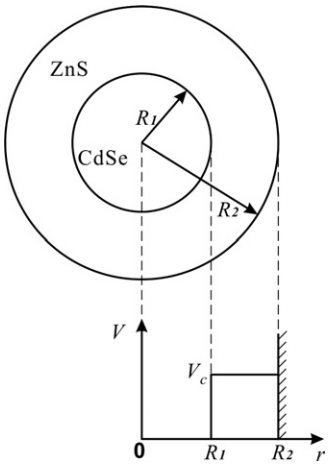

Figure 1. The core–shell CdSe/ZnS QD model and its schematic diagram of potential.

$$V_i(r) = \begin{cases} 0, & 0 < r \leqslant R_1 \\ V_c, & R_1 < r \leqslant R_2 \\ \infty, & r > R_2. \end{cases} \tag{3}$$

As the mass and the potential are spherically symmetric, the separation of radial and angular coordinates leads to

$$\Phi_{nlm}(r, \theta, \phi) = R_{nl}(r) Y_{lm}(\theta, \phi) \tag{4}$$

where $R_{nl}(r)$ is the radial wavefunction and $Y_{lm}(\theta, \phi)$ is the spherical harmonic. The spherical potential consists of three parts, and the radial eigenfunction $R_{nl}(r)$ consists of three parts too, corresponding to the position of the electron in the model. Consequently, to solve equation (1), two cases need to be distinguished.

In the region where $E > V_c$, the solution for the radial wavefunction $R_{nl}(r)$ is a linear combination of a spherical harmonic Bessel function $j_l(x)$ and a spherical harmonic Neumann function $n_l(x)$ [15, 16]

$$R_{nl}(r) = \begin{cases} A_1 j_l(k_{nl,1} r) + B_1 n_l(k_{nl,1} r) & r \leqslant R_1 \\ A_2 j_l(k_{nl,2} r) + B_2 n_l(k_{nl,2} r) & R_1 < r \leqslant R_2 \\ 0 & r > R_2 \end{cases} \tag{5}$$

with

$$k_{nl,1} = \sqrt{2m_1^* E/\hbar^2} \tag{6}$$

$$k_{nl,2} = \sqrt{2m_2^* (E - V_c)/\hbar^2}. \tag{7}$$

A_1, A_2, B_1 and B_2 are normalized constants.

The boundary conditions for the function are [17, 18]

$$R_{nl,1}(R_1) = R_{nl,2}(R_1) \tag{8}$$

$$\frac{1}{m_1^*} \frac{\mathrm{d}R_{nl,1}}{\mathrm{d}r}\bigg|_{r=R_1} = \frac{1}{m_2^*} \frac{\mathrm{d}R_{nl,2}}{\mathrm{d}r}\bigg|_{r=R_1}. \tag{9}$$

The wavefunction is limited when $r \to 0$, $B_1 = 0$ and the wavefunction starts to vanish rapidly when $r \to \infty$, namely

$$R_{nl,2}(R_2) = 0. \tag{10}$$

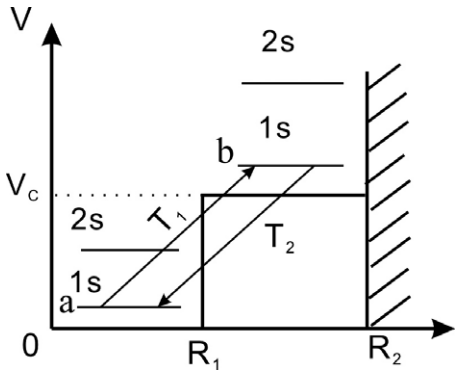

Figure 2. Description of the electron transition process.

The wavefunction must satisfy the normalization condition

$$\int_0^{r_1} r^2 R_{nl,1}^* R_{nl,1}\,\mathrm{d}r + \int_{r_1}^{r_2} r^2 R_{nl,2}^* R_{nl,2}\,\mathrm{d}r = 1. \tag{11}$$

The four coefficients A_1, A_2, B_2 and E can be obtained by solving equations (8)–(11), then the wavefunction and eigen-energy are obtained.

In the region where $E < V_c$, the radial wavefunction will stay the same as the above where $r \leqslant R_1$ and $r > R_2$, but in the range of $R_1 < r \leqslant R_2$ the radial wavefunction is a linear combination of two Hankel functions $h_l^{(+)}$ and $h_l^{(-)}$

$$R_{nl}(r) = \begin{cases} A_1' j_l(k_{nl,1}r) + B_1' n_l(k_{nl,1}r) & r \leqslant R_1 \\ A_2' h_l^{(+)}(\mathrm{i}k_{nl,2}r) + B_2' h_l^{(-)}(\mathrm{i}k_{nl,2}r) & R_1 < r \leqslant R_2 \\ 0 & r > R_2 \end{cases} \tag{12}$$

with

$$k_{nl,2} = \sqrt{2m_2^*(V_c - E)/\hbar^2}. \tag{13}$$

It is obvious that $B_1' = 0$ and A_1', A_2', B_2' and E can be obtained by solving equations (8)–(11).

Of course, we can restrict the calculations to the 1s state inside the well ($l = m = 0$) and the 1s state outside the well ($l = 1, m = 0$). These calculations can be performed not only for electrons but also for holes.

We consider a single photon transition process in a two-level system (figure 2). Due to the fact that the radius of the semiconductor QD is kept smaller than its Bohr radius, the kinetic energy of those charge carriers is much bigger than the Coulomb interaction energy between electrons and holes. The energy of electrons and holes is quantized. (The exciton Bohr radius is 5.6 nm in bulk CdSe materials.) Therefore the Coulomb interaction term can be neglected, and we can use the particle-in-the-box-model (PBM) for analysis.

The Hamiltonian for this system while it is irradiated with a femtosecond laser pulse can be written as:

$$H = H^{\mathrm{M}} + H^{\mathrm{I}} + H^{\mathrm{R}} \tag{14}$$

where

$$H^{\mathrm{M}} = \begin{bmatrix} E_a & 0 \\ 0 & E_b \end{bmatrix} \tag{15}$$

$$H^{\mathrm{I}} = -\mu \cdot E_0 = \begin{bmatrix} 0 & -\mu_{ab}E_0 \\ -\mu_{ba}E_0 & 0 \end{bmatrix} \tag{16}$$

$$[\,H^{\mathrm{R}},\quad \rho\,] = \mathrm{i}\hbar \begin{pmatrix} \rho_{aa}\gamma_a & \rho_{ab}\gamma_{ab} \\ \rho_{ba}\gamma_{ab} & \rho_{bb}\gamma_b \end{pmatrix} \tag{17}$$

where H^{M} is the unperturbed Hamiltonian, E_a and E_b are the energy eigenvalues of a and b levels, respectively, H^{I} is the interaction Hamiltonian between the light field and the QD, E_0 is the electric component of the polarized light field, μ is the electric dipole moment of transition, and

$$\mu = \begin{pmatrix} 0 & \mu_{ab} \\ \mu_{ba} & 0 \end{pmatrix} \tag{18a}$$

in which

$$\mu_{ab} = \langle \Phi_a | -er | \Phi_b \rangle. \tag{18b}$$

H^{R} is the relaxation Hamiltonian, γ_a and γ_b are the longitudinal relaxation velocities of energy levels a and b and γ_{ab} is the transverse relaxation velocity.

The Liouville equation for the density matrix is

$$\mathrm{i}\hbar \frac{\partial \rho}{\partial t} = [\,H^{\mathrm{M}} + H^{\mathrm{I}},\quad \rho\,] + \mathrm{i}\hbar \left(\frac{\partial \rho}{\partial t}\right)_{\text{damping}}. \tag{19}$$

Then, the optical Bloch equation can be derived using the rotating-wave approximation and slowly varying amplitude approximation:

$$\dot{u} = \Delta v - \gamma_{ab} u = \Delta v - \frac{u}{T_2} \tag{20a}$$

$$\dot{v} = -\Delta u + \chi w - \gamma_{ab} v = -\Delta u + \chi w - \frac{v}{T_2} \tag{20b}$$

$$\dot{w} = -\chi v - \gamma [w - w_0] = -\chi v - \frac{w - w_0}{T_1} \tag{20c}$$

where u, v and w are the three parameters of the Bloch vector $M \equiv (u, v, w)$. χ is the Rabi frequency, in the case of near-resonant excitation,

$$\chi = \frac{\mu_{ab} E_0}{\hbar} \tag{21}$$

where $\gamma = 1/T_1$, $\gamma_{ab} = 1/T_2$; T_1 and T_2 are the longitudinal and transverse relaxation times, respectively, of the energy level. Δ is the deviation of frequency between the irradiating light field frequency and the resonant frequency of the material; usually it is zero in the special case of a near-resonant excitation by a polarized quasi-monochromatic field.

We can solve these three equations, (20*a*), (20*b*) and (20*c*), and the analytical solution is as follows:

$$\begin{pmatrix} u \\ v \\ w \end{pmatrix} = \mathrm{e}^{\gamma t} w_0 \begin{pmatrix} \frac{\chi \Delta}{g^2}(1 - \cos gt) \\ \frac{\chi}{g} \sin gt \\ 1 - \frac{\chi^2}{g^2}(1 - \cos gt) \end{pmatrix} \tag{22}$$

where $g = \sqrt{\chi^2 + \Delta^2}$ is the rotational velocity of processional motion.

The induced effective polarization in the QD can be calculated as

$$P_{\text{eff}} = -\mu_{ab} \int_{-\infty}^{\infty} v \, \mathrm{d}v_z = -\frac{\mu_{ab}\chi}{v_{\mathrm{r}}\sqrt{\pi}} \mathrm{e}^{-\gamma t'} (N_a^0 - N_b^0) \int_{-\infty}^{\infty} \exp(-v_z^2 / v_{\mathrm{r}}^2) \frac{\sin gt'}{g} \, \mathrm{d}v_z \tag{23}$$

where v_z is the velocity component of the thermal motion of an atom in the direction of the laser pulse. v_{r} is the root-mean-square value of the velocity of the thermal motion of an atom and $N_a^0 - N_b^0$ is the difference ion the particle population in unit volume between two energy levels in the initial state.

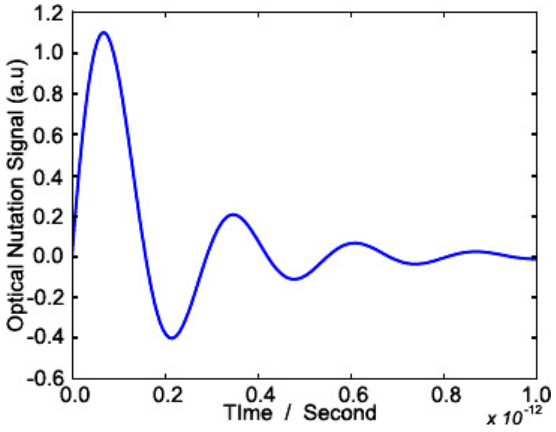

Figure 3. The optical nutation signal under the condition that $R_1 = 4.5$ nm, $R_2 = 5.5$ nm and the resonant wavelength $\lambda = 1075$ nm.

The numerical solution of the induced polarization can be obtained by solving equations (22) and (23). The expression of the transient nutation signal can be obtained as

$$I_S = -\tfrac{1}{2} E_0 \omega L P_{\text{eff}}(t - \tau) \tag{24}$$

where ω is the frequency of the laser pulse, L is the thickness of the sample and τ is the time that the laser pulse takes to cross the sample.

3. Results and discussion

The QD is excited near-resonantly by a 150 fs pulsed laser, whose electric field amplitude $E_0 = 5 \times 10^7$ V m^{-1}. It is under a weak excitation regime and at low temperature [19].

The parameters used in the calculation are chosen as follows: $m^*_{\text{e,CdSe}} = 0.13\, m_0$, $m^*_{\text{e,ZnS}} = 0.28\, m_0$ (m_0 is the rest mass of electron), $V_c = 1.03$ eV [16, 20], the relaxation times $T_1 = T_2 = 300$ fs and $N^0_a - N^0_b = 5 \times 10^{24}$ m^{-3} [21, 22].

First, we have calculated the electric transition dipole moment induced by 1s (inside the well)–1s (outside the well) transition using equation (18) under the condition that $\mu_{ab} = 5.101 \times 10^{-29}$ C m, $R_1 = 4.5$ nm and $R_2 = 5.5$ nm. The optical nutation signal is obtained from equations (23) and (24), and is shown in figure 3.

It is shown in figure 3 that the nutation signal decays rapidly: it arises due to the transient polarization induced in the QD and decays for the reason that the absorption coefficient is directly proportional to the population difference of the electrons, which is decreasing rapidly. Similar decay behaviour for quantum wires and micro-cavity was reported in [13, 14, 23–25].

Secondly, when one of R_1 and R_2 remains steady and the other changes, there are some interesting phenomena concerning the variation of the nutation signal.

Figure 4 illustrates that when R_2 varies from 4.8 to 7.8 nm and $R_1 = 4.8$ nm is kept steady the intensity of the optical nutation signal increases first and then decreases, and the Rabi frequency of the oscillation increases first and then decreases too. This behaviour reveals that, with growth in the thickness of the shell while the size of the core does not change, there is an optimum structure and size for the optical nutation phenomenon. It means the nonlinear optical properties of the heterostructure particles are dependent on its size and structure.

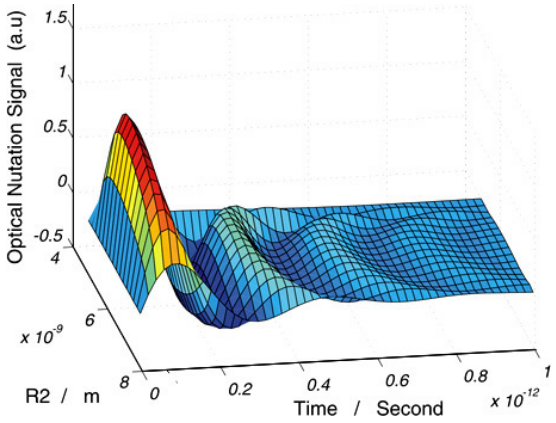

Figure 4. The optical nutation signal changes with the size of R_2 when $R_1 = 4.8$ nm.

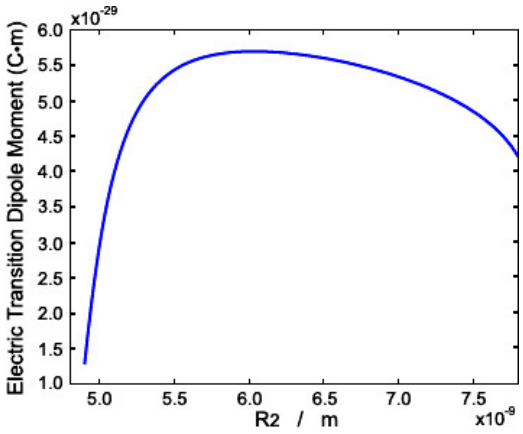

Figure 5. The electric transition dipole moment as a function of R_2 ($R_1 = 4.8$ nm kept steady).

According to equations (21), (23) and (24), the immediate cause for this is the increase or decrease in the electric transition dipole moment of the heterostructure particles with the change of size and structure. The electric transition dipole moment has been calculated numerically and the result is shown in figure 5. It shows that there is a process of growth first and then decline. The maximum of the electric transition dipole moment is found under the condition that $R_2 = 6.05$ nm and $R_1 = 4.8$ nm.

This phenomenon can be explained by QSCE theory. There are two factors that influence the variation of the electric transition dipole moment, energy spacing between these two energy levels and charge distribution. It can be seen from figure 6 that because the growth of the thickness of the shell weakens the QSCE outside the well, the energy spacing between two 1s states decreases [26]. This will lead to an increase in the electric transition dipole moment [15].

However, figure 7 shows that the value of $\int_0^{R_1} r^2 R^* R \, \mathrm{d}r$ decreased with growth of R_2, i.e. the probability of occurrence of electrons appearing inside the core was reduced with the growth of R_2. The reason for this is that the QSCE inside the shell diminished and that inside the core remained steady; therefore more electrons will exist inside the shell with the growth

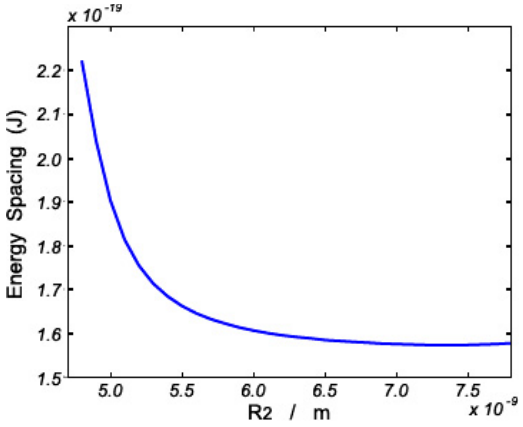

Figure 6. The energy spacing between two 1s states as a function of R_2 ($R_1 = 4.8$ nm kept steady).

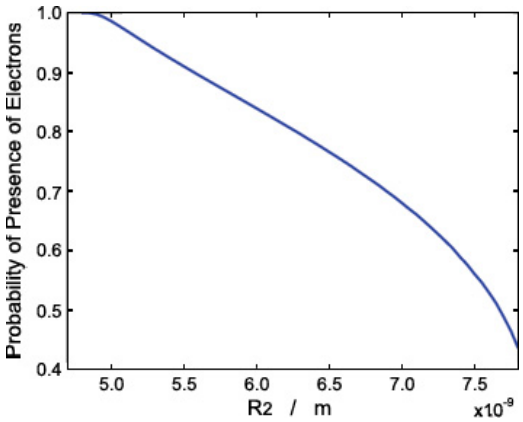

Figure 7. The probability of electrons presenting inside the core as a function of R_2 ($R_1 = 4.8$ nm kept steady).

of R_2. This will prevent electrons from relaxing to the 1s state inside the well and diminish the electric transition dipole moment.

So there exists competition between these two factors, and the result is that the electric transition dipole moment increases first and decreases later. The optimum structure and size for the optical nutation phenomenon is $R_2 = 6.05$ nm when $R_1 = 4.8$ nm is kept steady.

The same thing happens when R_1 changed and $R_2 = 5.5$ nm kept steady. It is shown in figure 8 that, when $R_2 = 5.5$ nm, with the increase of R_1 the electric transition dipole moment element μ_{ab} between these two 1s states increases first then decreases. The reason is as same as that given above: the growth of the inner radius R_1 will weaken the QSCE inside the core and strengthen the QSCE inside the shell, the energy spacing between these two 1s states will increase and the occurrence probability that electrons will appear inside the core will be enhanced. The former factor will reduce μ_{ab} and the latter factor will enhance μ_{ab}. Therefore, the electric transition dipole moment increases first and decreases later because of the competition between these two factors.

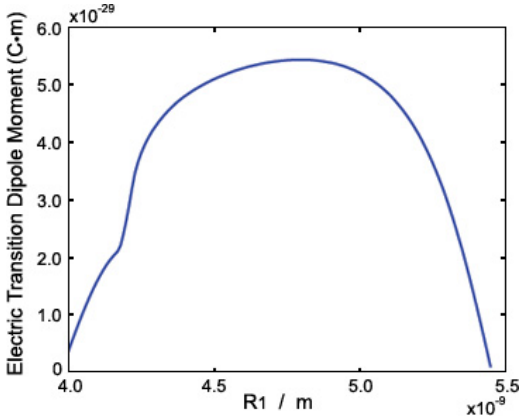

Figure 8. The electric transition dipole moment as a function of R_1 ($R_2 = 5.5$ nm kept steady).

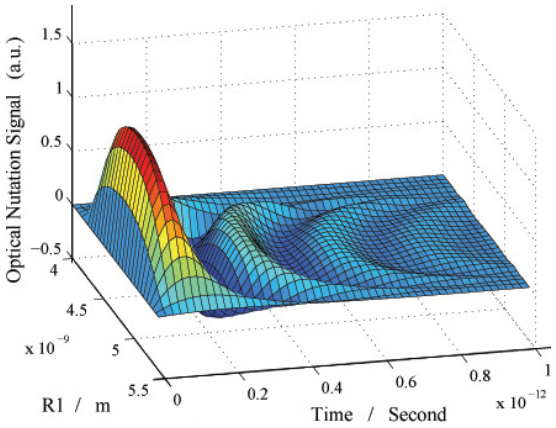

Figure 9. The optical nutation signal as a function of the size of R_1 ($R_2 = 5.5$ nm kept steady).

It can be seen from figure 9 that the optical nutation signal varies in the same way as for the case of changing R_2 when R_1 kept steady: with the growth in size of the core when R_2 is kept steady, the Rabi frequency of the oscillation increases first and decreases later, and the intensity of the optical nutation signal increases first and decreases later too. The optimum structure and size for the optical nutation phenomenon in this system is $R_1 = 4.75$ nm when $R_2 = 5.5$ nm kept steady.

4. Conclusion

In conclusion, a theoretical analysis of the optical nutation signal of a core–shell CdSe/ZnS QD has been presented in this paper based on the effective-mass approximation and the two energy levels model. In particular the influence of the change of the size parameter of the QDs on the optical nutation signals of the 1s (inside the well)–1s (outside the well) transition of electrons has been investigated. The results of numerical calculation reveal that the nutation signals are greatly dependent on the size and structure of the QD. The reasons for this have been discussed in terms of the theory of QSCE.

It would be much better if there were experimental results available for the optical transient nutation induced in CdSe/ZnS core–shell quantum dot sample so that a comparison could be

made between the theoretical and experimental results. Unfortunately, to date there have been no reports of such experimental work on optical nutation in CdSe/ZnS core/shell quantum dots. In the analysis of size-dependent optical nutation in core–shell quantum dots, only the laser field–quantum dot interaction was considered, i.e. other interactions, especially the Coulomb interaction between electrons and holes, have not been taken into account. We will include this in future work in order to improve the considered approximation.

Acknowledgment

This work was financially supported by the National Natural Foundation of China under grant no. 10534030.

References

[1] Haase M A, Qiu J, DePuydt J M and Cheng H 1991 *Appl. Phys Lett.* **59** 1272
[2] Taniguchi S *et al* 1996 *Electron. Lett.* **32** 552
[3] Zheng Z H *et al* 1995 *Japan. J. Appl. Phys.* **34** 56
[4] Uematsu T, Kimura J and Yamaguchi Y 2004 *Nanotechnology* **15** 822
[5] Bryant G W and Band Y B 2001 *Phys. Rev.* B **63** 115304
[6] Kyrychenko F V and Kossut J 2000 *Phys. Rev.* B **61** 4449
[7] Siarkos A and Runge E 2000 *Phys. Rev.* B **61** 16854
[8] Azad Malik M, O'Brien P and Revaprasadu N 2002 *Chem. Mater.* **14** 2004
[9] Hikmet R A M *et al* 2003 *J. Appl. Phys.* **93** 3509
[10] Hocker G B and Tang C L 1968 *Phys. Rev. Lett.* **21** 591
[11] Shoemaker R L and Van Stryland E W 1976 *J. Chem. Phys.* **64** 1733
[12] Singh K, Sen P and Sen P K 1989 *IEEE J. Quantum Electron.* **25** 67
[13] Kapoor S, Kumar J and Sen P K 2004 *J. Appl. Phys.* **95** 4833
[14] Sen P K, Bafna M K and Gupta S K 2004 *J. Appl. Phys.* **96** 5552
[15] Schooss D, Mews A, Eychmüller A and Weller H 1994 *Phys. Rev.* B **49** 17072
[16] Haus J W, Zhou H S, Honma I and Komiyama H 1993 *Phys. Rev.* B **47** 1359
[17] Ben Daniel D J and Duke C B 1966 *Phys. Rev.* **152** 683
[18] Brus L E 1983 *J. Chem. Phys.* **79** 5566
[19] Lindberg M and Koch S W 1988 *Phys. Rev.* B **38** 3342
[20] Nethercot A N 1974 *Phys. Rev. Lett.* **33** 1088
[21] Wang G and Guo K 2001 *J. Phys.: Condens. Matter* **13** 8197
[22] Woggon U, Gindele F and Langbein W 2000 *Phys. Rev.* B **61** 1935
[23] Bongiovanni G *et al* 1997 *Phys. Rev.* B **55** 7084
[24] Kapoor S, Kumar J and Sen P K 2005 *Phys. Status Solidi* b **242** 1650
[25] Berger J D, Lyngnes O, Gibbs H M, Khitrova G, Nelson T R, Lindmark E K, Kavokin A V, Kaliteevski M A and Zapasskii V V 1996 *Phys. Rev.* B **54** 1975
[26] Liu L, Li J and Xiong G 2005 *Physica* E **25** 466